SCIREA Journal of Electrics, Communication and Automatic Control

http://www.scirea.org/journal/ECAC

December 21, 2016

Volume 1, Issue 2, December 2016

# Modeling the Effects of Emitter Doping Non-uniformity on the Internal Quantum Efficiency of Si-Drift Solar Cells

**Md. Yasin Javed Chowdhury[1], Md. Imrul Basher Chowdhury[2] and Md. Iqbal Bahar Chowdhury[3]**

[1]Sonali Bank Limited, Ramna Branch, Dhaka, Bangladesh

[2]Ahsanullah University of Science and Technology, Dhaka, Bangladesh

[3]United International University, Dhaka, Bangladesh

## Abstract

The introduction of non-uniform doping profile in the quasi-neutral regions of a solar cell helps achieve better performance parameters such as higher conversion efficiency and improved current-voltage characteristics. However, a number of non-ideal effects becomes dominant as the doping level is increased; the transport parameters (i.e. mobility and lifetime) become doping and field dependent, the space-dependency of the bandgap narrowing becomes significant and the Auger recombination mechanism becomes dominant. These effects adversely affect the internal quantum efficiency and hence, need to be considered with great care. Unfortunately, owing to the evolving mathematical intractability, all these effects are not considered simultaneously in the existing models. This work focuses to develop an analytical model for a drift-field Si-solar cell with non-uniformly and heavily doped emitter region where the mathematical intractability problem has been resolved by employing an elegant approximation technique called "Exponential Approximation Technique". The developed model shows that the drift-field solar cells have significantly higher internal

quantum efficiency over the uniformly-doped Si-solar cells, particularly for high energy photons.

**Keywords:** Drift-field solar cell, internal quantum efficiency, non-uniform doping profile.

## 1. Introduction

In order to obtain higher fill factor and higher conversion efficiency of a solar cell, its shape of current-voltage characteristics need to be improved. This improvement can be made by decreasing the reverse saturation currents in the quasi-neutral regions (emitter and base) owing to the diode action of the solar cell. In the drift field (DF) solar cells [1] this reduction of reverse saturation currents can be obtained by appropriate introduction of non-uniform and heavy doping levels in the bulk emitter-base regions to develop an electric field therein in accordance with the built-in field developed in the depletion region. The strength of the developed electric field is determined by the logarithmic gradient of the doping profile. Therefore, the peak doping levels for modern DF solar cells need to be higher to obtain stronger electric field and hence, higher conversion efficiency.

However, heavy and non-uniform doping levels introduce a number of non-ideal effects which include the space dependency of the energy band-gap narrowing and the carrier transport parameters (mobility and lifetime), the electric field dependency of the carrier mobility and the dominance of the Auger recombination mechanisms over the Shockley-Read-Hall (SRH) recombination mechanism. All these effects degrade the performance parameters of the DF solar cells far from the expectation and hence, need to be analyzed carefully. However, consideration of all these effects makes the analytical modeling mathematically intractable and the conventional models [2-7] found in the literature, therefore, failed to incorporate all these effects. Verhoef and Sinke [8, 9] considered the doping dependence of the transport parameters and the bandgap narrowing effects in their models; but they failed to incorporate the SRH and the Auger recombination simultaneously owing to the evolving mathematical complexity; instead, they considered the SRH recombination for the doping levels $\leq 5 \times 10^{18}\ cm^{-3}$ and the Auger recombination for the higher doping levels as the dominant recombination mechanism. Moreover, their model is applicable for the dark saturation current only, not for the internal quantum efficiency. Later, M. R. Huqe et. al [10] resolved this mathematical intractability by employing an elegant exponential approximation

technique and hence, developed an analytical model for the dark saturation current in the non-uniformly and heavily doped p-type base region. However, this model is not applicable for analyzing the internal quantum efficiency. Indeed, there is no model in the literature which analyzes the effects of the non-uniformity of the emitter doping profile on the internal quantum efficiency. Therefore, the objective of this work is to investigate the effects of emitter doping non-uniformity by developing an analytical model of the internal quantum efficiency of DF solar cells having non-uniformly and heavily doped emitter region along with a uniformly doped base region and also, considering all of the above-mentioned non-ideal effects.

## 2. Analysis

### 2.1 Basic Equations and Physical Models

In order to determine the photocurrent generated within the non-uniformly doped emitter region for the development of an analytical model of the internal quantum efficiency of a Si-drift solar cell, the solution of the following equations are necessary.

$$J_p(x) = qp(x)\mu_p(x)E(x) - qD_p\frac{dp}{dx} \quad (1)$$

$$\frac{dJ_p}{dx} = -q\left(R_p - G_p\right) \quad (2)$$

where, $J_p(x)$ is the hole current density, $p(x)$ is the hole concentration, $\mu_p$ ($D_p$) is the hole mobility (diffusivity), $R_p$ is the recombination rate, $G_p$ is the generation rate, $E(x)$ is the electric field acting on the holes and q is the electronic charge. Since the emitter region is non-uniformly and heavily doped, the band-gap narrowing effects, the doping dependence of the carrier transport parameters (i.e. the mobility and the lifetime) and the presence of both the Shockley-Read-Hall (SRH) and the Auger recombination mechanisms have to be considered. Therefore, the physical models to describe these non-ideal effects are necessary.

The band-gap narrowing (BGN) effects are manifested mainly in the doping dependence of the effective intrinsic carrier concentration ($n_{ie}$). These changes in $n_{ie}$ can be modeled as [11]

$$n_{ie}^2 = n_{i0}^2\left[\frac{N_d(x)}{N_{ref}}\right]^{\gamma_2} \quad (3)$$

with $n_{i0} = 1.194 \times 10^{10}$ cm$^{-3}$, $N_{ref} = 1.3 \times 10^{17}$ cm$^{-3}$ and $\gamma_2 = 0.5355$ are the fitting parameters determined in [11] and $N_d(x)$ is the emitter doping density. The electric field $E(x)$ introduced

in the emitter region is modified by the BGN effects through the position dependence of $n_{ie}$ as [12]

$$\frac{E(x)}{V_T} = -\frac{d}{dx}\ln N_d(x) + \frac{d}{dx}\ln\, n_{ie}^2(x) \tag{4}$$

where $V_T$ is the thermal voltage. The doping-dependence of the low-field hole mobility can be expressed as [13]

$$\mu_p(x) = \frac{D_p(0)}{V_T}\left[\frac{N_d(x)}{N_{m,ref}}\right]^{-\gamma_3} \tag{5}$$

with $D_p(0)$ = 12.5727 $cm^2$ $(V.s)^{-1}$, $N_{m,ref}$ = 1× $10^{17}$ $cm^{-3}$, and $\gamma_3$ = 0.38 are the fitting parameters determined in [13]. The doping dependent SRH recombination rate ($R_{SRH}$) and Auger recombination rate ($R_{Auger}$), under steady-state condition, are given by

$$R_{SRH} = \frac{p}{\tau_{ps}}, \quad R_{Auger} = \frac{p}{\tau_{pa}} \tag{6}$$

$$\tau_{ps}(x) = \frac{\tau_{p0}}{1+\frac{N_d(x)}{N_{0,ref}}}, \quad \tau_{pa}(x) = \frac{1}{C_{An}N_d^2} \tag{7}$$

where, $\tau_{ps}$, $\tau_{pa}$ are the position dependent carrier lifetime for the SRH recombination [14] and the Auger recombination respectively, $N_{0,ref}$ = 7.1 × $10^{15}$ $cm^{-3}$ and $\tau_{p0}$ = 3.52 × $10^{-4}$ sec are the fitting parameters for the SRH recombination determined in [15] and $C_{An}$ is the Auger coefficient for holes given by [16]

$C_{An}$ = 0.67 × $10^{-31}$ + 8.16 × $10^{-34}$ T – 2.44 × $10^{-37}$ $T^2$

where T is the ambient temperature in degree Kelvin. The steady-state generation rate due to optical illumination $G_p$ at any wavelength $\lambda$ is given by

$$G_p(\lambda) = \frac{\alpha(\lambda)\lambda I_0(\lambda)}{hc}e^{-\alpha(\lambda)x} = \alpha(\lambda)G_0(\lambda)e^{-\alpha(\lambda)x} \tag{8}$$

where $I_0$ is the solar irradiance at the emitter surface and α is the absorption coefficient of silicon at a given wavelength (λ), h is the Plank's constant, c is the velocity of light and $G_0(\lambda) = \frac{\alpha(\lambda)\lambda I_0(\lambda)}{hc}$. Finally, the hole current continuity equation [Eqn. (2)] can be furnished as

$$\frac{dJ_p}{dx} = -\frac{qp}{\tau_{p,eff}} + q\alpha(\lambda)G_0(\lambda)e^{-\alpha(\lambda)x} \tag{9}$$

where $\tau_{p,eff}$ is the effective hole lifetime given by $\frac{1}{\tau_{p,eff}} = \frac{1}{\tau_{ps}} + \frac{1}{\tau_{pa}}$

## 2.2 Model Derivation:

The equations (1) and (9) can be refurnished using Eqns. (4) to (8) as

$$\frac{d}{dx}\left(\frac{pN_d}{n_{ie}^2}\right) = -\frac{J_p}{qD_p}\left(\frac{N_d}{n_{ie}^2}\right) \tag{10}$$

$$\left(\frac{N_d\tau_{p,eff}}{qn_{ie}^2}\right)\frac{dJ_p}{dx} = -\frac{pN_d}{n_{ie}^2} + q\alpha G_0 e^{-\alpha x} \times \left(\frac{N_d\tau_{p,eff}}{qn_{ie}^2}\right) \tag{11}$$

Combining the above equations results in a second order differential equation (DE) of $J_p(x)$ as

$$\frac{d^2J_p}{dx^2} + \left[\frac{d}{dx}ln\left(\frac{N_d\tau_{p,eff}}{qn_{ie}^2}\right)\right]\frac{dJ_p}{dx} - \frac{J_p}{D_p\tau_{p,eff}} = \quad -q\alpha G_0 e^{-\alpha x}\left[\frac{d}{dx}ln\left(\frac{N_d\tau_{p,eff}}{qn_{ie}^2}\right) - \alpha\right] \tag{12}$$

Using Eqn. (4), the above equation can be rewritten as

$$\frac{d^2J_p}{dx^2} + \left[\frac{E}{V_T} - \frac{d}{dx}ln\left(\frac{1}{\tau_{p,eff}}\right)\right]\frac{dJ_p}{dx} - \frac{J_p}{L_{p,eff}^2} = \quad -q\alpha G_0 e^{-\alpha x}\left[\frac{E}{V_T} - \frac{d}{dx}ln\left(\frac{1}{\tau_{p,eff}}\right) - \alpha\right] \tag{13}$$

where $L_{p,eff} = \sqrt{D_p\tau_{p,eff}}$ represents the effective diffusion length. The solution of the DE [Eqn. (13)] requires the doping profile used in the emitter. The exponential emitter doping profile used in this analysis can be expressed as

$$N_d(x) = N_d(0)e^{-\frac{\eta x}{W_e}} = N_d(0)u$$

where '$W_e$' is the width of the emitter region, $u = e^{-\frac{\eta x}{W_e}}$ represents the position dependence of the doping profile, $\eta = log\left[\frac{N_d(0)}{N_d(W_e)}\right]$ is the logarithmic slope of the doping profile and $N_d(0)$ and $N_d(W_e)$ are the emitter doping levels at x = 0 and $x = W_e$ respectively.

For the exponential doping profile, therefore, the electric field, the mobility and the lifetime of holes in the emitter region can be modified as

$$\frac{E}{V_T} = -\frac{\eta}{W_e}(1 - \gamma_2) \tag{14}$$

$$\frac{1}{qD_p} = \frac{1}{qD_p(0)}\left[\frac{N_d(x)}{N_{m,ref}}\right]^{\gamma_3} = F_h u^{\gamma_3} \tag{15}$$

$$\frac{1}{\tau_{ps}} = \frac{1}{\tau_{p0}} + \left[\frac{N_d(0)}{N_{0,ref}\tau_{p0}}\right]u \tag{16}$$

$$\frac{1}{\tau_{pa}} = [C_{An}N_d^2(0)]u^2 \tag{17}$$

Where, $F_h = \frac{1}{qD_p(0)}\left[\frac{N_d(0)}{N_{m,ref}}\right]^{\gamma_3}$. The DE given by Eqn. (13) can be written for the exponential doped emitter as

$$\frac{d^2J_p}{dx^2} + \left[-\frac{\eta}{W_e}(1 - \gamma_2) - \frac{d}{dx}ln\left(\frac{1}{\tau_{p,eff}}\right)\right]\frac{dJ_p}{dx} - \frac{J_p}{L_{p,eff}^2} = -q\alpha G_0 e^{-\alpha x}\left[-\frac{\eta}{W_e}(1 - \gamma_2) - \frac{d}{dx}ln\left(\frac{1}{\tau_{p,eff}}\right) - \alpha\right] \quad (18)$$

It is evident from the above Eqn. (18) that the DE is analytical intractable due to the presence of the position dependent effective lifetime ($\tau_{p,eff}$), which incorporates both the SRH and the Auger recombination lifetime. Verhoef and Simke [8, 9] separately considered these SRH and Auger recombination to resolve this intractability. In this work, however, using the exponential approximation technique [10], the terms $\frac{1}{\tau_{p,eff}}$and $\frac{1}{L_{p,eff}^2}$ can be approximated as a simple exponential given by $\frac{1}{\tau_{p,eff}} \equiv R_0 u^{k_p}$ and $\frac{1}{L_{p,eff}^2} \equiv L_0 u^{m_p}$ respectively, where $k_p$, $m_p$, $R_0$ and $L_0$ are defined according to the exponential approximation technique described in [10] as

$$k_p = \frac{1}{\eta} log\left[\frac{\frac{1}{\tau_{p,eff}(0)}}{\frac{1}{\tau_{p,eff}(W_e)}}\right], \quad m_p = \frac{1}{\eta} log\left[\frac{\frac{1}{L_{p,eff}^2(0)}}{\frac{1}{L_{p,eff}^2(W_e)}}\right]$$

$$R_0 = \frac{\eta k_p}{W_e} \times \frac{\int_0^{W_e} \frac{1}{\tau_{p,eff}(x)} dx}{1 - e^{-\eta k_p}}, \qquad L_0 = \frac{\eta m_p}{W_e} \times \frac{\int_0^{W_e} \frac{1}{L_{p,eff}^2(x)} dx}{1 - e^{-\eta m_p}}$$

Using these approximated exponentials, the DE of Eqn. (18) can be converted to a tractable form as

$$\frac{d^2J_p}{dx^2} - \frac{\eta}{W_e}(1 - \gamma_2 - k_p)\frac{dJ_p}{dx} - \frac{J_p}{L_0 u^{m_p}} = -q\alpha G_0 e^{-\alpha x}\left[-\frac{\eta}{W_e}(1 - \gamma_2 - k_p) - \alpha\right] \quad (19)$$

Using the boundary conditions at x = 0 and $x = W_e$ given by [8]

$$p(0) = -\frac{J_p(0)}{qS_p} \text{ and } p(W_e) = 0 \quad (20)$$

where $S_p$ is the surface recombination velocity of holes at the emitter surface, the solution of the DE [Eqn. (18)] gives the minority hole current density $J_p(x)$ as a linear combination of modified Bessel functions of the first kind $I_\beta$ and of the second kind $K_\beta$ of order β [Appendix]

$$J_p(x) = w(x)\left[(C_1' + v_1')I_\beta(X) + (C_2' + v_2')K_\beta(X)\right] \quad (21)$$

where all the variables and the constants are defined in the Appendix. The total photocurrent density at a given wavelength $\lambda$ can be obtained as [18]

$$J_{ph}(\lambda) = J_{ph,W_e}(\lambda) + J_{ph,depl}(\lambda) + J_{ph,0}(\lambda) \quad (22)$$

where $J_{ph,0}$ and $J_{ph,depl}$ are the electron photocurrent generated in the uniformly doped emitter region and in the depletion region respectively [17] and $J_{ph,We}$ is the photo-generated hole current density obtained using Eqn. (1) at the depletion edge i.e. $x = W_e$ in the emitter region. Finally, the wavelength dependent internal quantum efficiency can be obtained from

$$\eta_i = \frac{J_{ph}(\lambda)}{qG_0(\lambda)} \times 100\% \tag{23}$$

## 3. Results and Discussions

Based on the analytical model developed in this work simulations are carried out for a Si-drift solar cell with non-uniformly doped emitter and uniformly doped base and also, for a Si-solar cell with uniformly doped emitter and base. In this section, these simulation results are presented and then analyzed to investigate the effects of non-uniformity of the emitter doping on the internal quantum efficiency. For convenience, the model developed in this work for the drift solar cell is termed as the 'present model', whereas, the term 'previous model' refers to the model with uniformly-doped Si solar cell.

Figs. (1) to (3) provide a comparative picture of the internal quantum efficiency $\eta_i$ for the present and the previous models under various conditions. Two common observations can be made from all these figures. First-the internal quantum efficiency for the present model is higher than the previous model especially for the mid to high energy photons and second- the effect of surface recombination is reduced with the increase of the electric field. The non-uniformity of the emitter doping profile is such that it creates an electric field in the neutral emitter region in the same direction as the field in the depletion region. This field causes photo-generated carriers for mid to high-energy photons in the emitter region to pass with an increased velocity, thereby, increases the photo-current. On the other hand, the roughness of the surfaces is represented by the surface recombination velocity. The worse is the roughness of the surface, the higher is the carrier loss at the surface (the higher is the recombination occurred) and hence, the lower is the internal quantum efficiency. However, introduction or increase in the electric field in the quasi-neutral emitter region causes holes to drive away at a faster rate from the surface and lessens the probability of surface recombination resulting in the improvement in $\eta_i$.

Electric field introduced in the emitter region with the help of the non-uniform doping profile is directly related with the logarithmic gradient of the doping profile. Increase in the doping

level at the junction (at $x = W_e$) i.e. $N_d(W_e)$ causes this gradient and hence, the electric field to decrease. Therefore, with the increase in $N_d(W_e)$ while maintaining peak doping level at the surface ($x = 0$) results in lowering of the photocurrent and causes $\eta_i$ to decrease. This fact is evident from Fig. 1.

Fig. (2) shows that the internal quantum efficiency decreases with the increase of the surface recombination velocity at the emitter surface. Since surface recombination velocity causes carrier loss at the emitter surface, the more the surface recombination, the less will be the photocurrent generated in the emitter region and hence, the internal quantum efficiency.

Fig. (3) shows that increase in the emitter ($W_e$) width decreases the internal quantum efficiency. This is due to the fact that increase in the emitter width increases the probability of volume recombination (SRH and Auger) in the emitter region. Moreover, increase in $W_e$ decreases the logarithmic gradient of the doping profile thereby causing the electric field in the emitter region to decrease.

## 4. Conclusion

In this work the effects of the non-uniform emitter doping profile on the internal quantum efficiency of a drift-field solar cell have been investigated. In doing so, an analytical model has been developed that includes the non-ideal effects such as the bandgap narrowing effect, the doping dependency of the carrier mobility and the carrier lifetime and the presence of the Auger recombination mechanism in the emitter owing to the heavy doping levels. Judicious application of the exponential approximation technique makes resolve the resulting intractability of the governing differential equation. The simulation results obtained from the developed analytical model shows that the non-uniformity of the emitter doping profile not only increases the internal quantum efficiency for the mid to high energy photons, but also decreases the effect of surface recombination velocity. Therefore, this work will be useful in designing high efficiency solar cells by providing better physical insight.

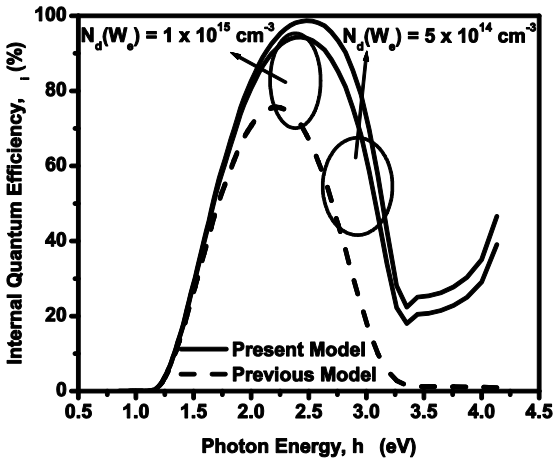


**Fig. 1: Internal quantum efficiency vs. photon energy for the present model and the previous model. Here, two emitter doping densities at x = $W_e$ of 5 × $10^{14}$ $cm^{-3}$ and 1 × $10^{15}$ $cm^{-3}$ are considered; $S_p$ = 1 × $10^6$ cm/sec, We = 0.5 μm and $N_d$ (0) = 1 × $10^{20}$ $cm^{-3}$.**

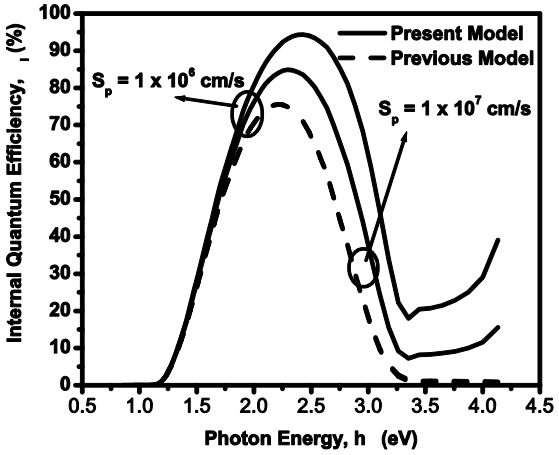


**Fig. 2: Internal quantum efficiency vs. photon energy for the present model and the previous model. Here, two surface recombination velocities of Sp = 1 × 106 cm/sec and Sp = 1 × 107 cm/sec are considered; We = 0.5 μm and Nd (0) = 1 × 1020 cm–3 and Nd (We) = 1 × 1015 cm–3.**

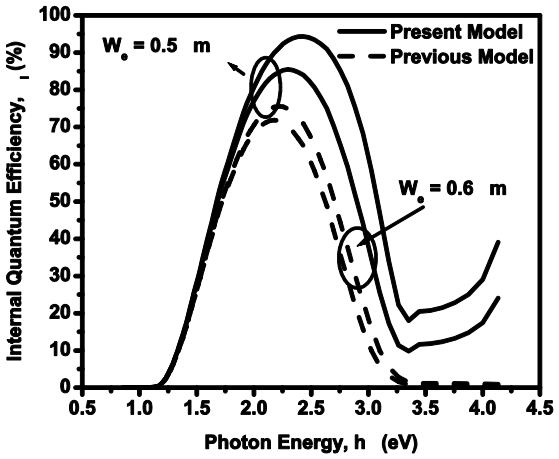


**Fig. 3: Internal quantum efficiency vs. photon energy for the present model and the previous model. Here, two emitter widths of 0.5 μm and 0.6 μm are considered; Sp = 1 × 106 cm/sec, Nd (0) = 1 × 1020 cm–3 and Nd (We) = 1 × 1015 cm–3.**

## Appendix

### Solution of the DE

Letting $J_p(x) = v(x)w(x)$ converts the second order DE [Eqn. (18)] to

$$\frac{d^2v}{dx^2} + \left[\frac{2}{w}\frac{dw}{dx} + G_1\right]\frac{dv}{dx} + \frac{1}{w}\left[\frac{d^2w}{dx^2} + G_1\frac{dw}{dx} - \left(\frac{u^{m_p}}{L_{p,eff}^2}\right)w\right]v =$$

$$-q\alpha G_0\frac{G_2}{w} \tag{24}$$

Where $G_1 = -\frac{\eta}{W_e}(1 - \gamma_2 - k_p)$ and $G_2 = -\frac{\eta}{W_e}(1 - \gamma_2 - k_p) - \alpha$. Letting $\frac{2}{w}\frac{dw}{dx} + G_1 = 0$ gives w(x) and Eqn. (24) as

$$w(x) = u^{-\left(\frac{1-\gamma_2-k_p}{2}\right)} \tag{25}$$

$$\frac{d^2v}{dx^2} - \left[\frac{G_1^2}{4} + \frac{u^{m_p}}{L_{p,eff}^2}\right]v = -q\alpha G_0\frac{G_2}{w} \tag{26}$$

Letting $\frac{1}{L_{p,eff}^2}u^{m_p} = z^2$converts Eqn. (26) into a non-homogeneous modified Bessel Equation as

$$\frac{d^2v}{dX^2} + \frac{1}{X}\frac{dv}{dX} - \frac{1}{X^2}[\beta^2 + X^2]v = -q\alpha G_0\frac{G_2}{wz^2} \tag{27}$$

where, $\beta = \frac{1-\gamma_2-k_p}{m_p}$ is the order of the modified Bessel equation and $X = \frac{2W_e}{\eta m_p} z = b_0 z$. The solution of the DE given by Eqn. (27) provides v(X) as a linear combination of the modified Bessel function of first and second kind [$I_\beta(X)$ and $K_\beta(X)$, respectively] as

$$v(X) = (C_1' + v_1')I_\beta(X) + (C_2' + v_2')K_\beta(X) \tag{28}$$

where $v_1', v_2'$ are obtained due to the non-homogeneity of the DE using the 'Method of Undetermined Coefficients' described in the standard calculus textbooks and can be expressed as

$$v_1'(x) = q\alpha G_0 \int_{x=0}^{x=W_e} b_0 K_\beta(X) \frac{G_2}{w} dx = q\alpha G_0 v_1(x)$$

$$v_2'(x) = -q\alpha G_0 \int_{x=0}^{x=W_e} b_0 I_\beta(X) \frac{G_2}{w} dx = q\alpha G_0 v_2(x)$$

The hole current density $J_p(x)$ in the emitter region and its derivative $\frac{dJ_p}{dx}$ then can be expressed as

$$J_p(x) = w(x)\left[(C_1' + v_1')I_\beta(X) + (C_2' + v_2')K_\beta(X)\right] \tag{29}$$

$$\frac{dJ_p}{dx} = -w(x)[(C_1' + v_1')A_x + (C_2' + v_2')B_x] \tag{30}$$

Where $A_x = z\frac{dI_\beta}{dx} - \frac{I_\beta}{2}\left[\frac{\eta}{W_e}\left(1-\gamma_2-k_p\right)\right]$ and $B_x = z\frac{dK_\beta}{dx} - \frac{K_\beta}{2}\left[\frac{\eta}{W_e}\left(1-\gamma_2-k_p\right)\right]$.

The constants $C_1'$ and $C_2'$can be determined using the boundary conditions $p(0) = -\frac{J_p(0)}{qS_p}$and $p(W_e) = 0$ [8] in Eqn. (30), and are given by

$$C_1' = -q\alpha G_0 C_1 = -q\alpha G_0 \left[\frac{C_0 B_w - C_w B_0}{A_0 B_w - A_w B_0}\right] \text{ and } C_2' = q\alpha G_0 C_2 = q\alpha G_0 \left[\frac{C_0 A_w - C_w A_0}{A_0 B_w - A_w B_0}\right]$$

where $A_0 = A_x(0) + \frac{I_\beta(0)}{S_p \tau_{p,eff}(0)}$, $B_0 = B_x(0) + \frac{K_\beta(0)}{S_p \tau_{p,eff}(0)}$, $C_0 = \frac{1}{w(0)}$ and $A_w = A_{xw}(W_e)$, $B_w = B_x(W_e)$, $C_w = A_x(W_e)v_1(W_e) - B_x(W_e)v_2(W_e) + \frac{e^{-\alpha W_e}}{w(W_e)}$. Finally, the hole current density at the depletion edge can be arranged as

$$J_p(W_e) = q\alpha G_0 w_w\left[(-C_1 + v_{1w})I_{\beta w} + (C_1 - v_{2w})K_{\beta w}\right]$$

where 'w' in the subscript indicates value at $x = W_e$.

## References


[1] M. Wolf, "Drift fields in photovoltaic solar energy converter cells," *Proc. IEEE,* vol. 51, no. 5, pp. 674-693, May 1963.

[2] S. Kaye and G. P. Rolik, "Optimum bulk drift-field thicknesses in solar cells," *IEEE Trans. Electron Devices,* vol. 13, no. 7, pp. 563-570, Jul. 1966.

[3] W. M. Bullis, "Influence of mobility and lifetime variations on drift-field effects in silicon-junction devices," *IEEE Trans. Electron Devices,* vol. 14, no. 2, pp. 75-81, Feb. 1967.

[4] R. V. Overstraeten and W. Nuyts, "Theoretical investigation of the efficiency of drift-field solar cells," *IEEE Trans. Electron Devices,* vol. 16, no. 7, pp. 632-641, Jul. 1969.

[5] F. A. Lindholm and Y. H. Chen, "Current-voltage characteristic for bipolar p-n junction devices with drift fields, including correlation between carrier lifetimes and shallow-impurity concentration," *J. Appl. Phys.*, vol. 53, no. 12, pp. 8863-8866, Dec. 1982.

[6] J. A. Del Alemo and R. M. Swanson, "The Physics and Modeling of Heavily Doped Emitters," *IEEE Trans. Electron Devices*, vol. 31, no. 12, pp. 1878-1888, Dec. 1984.

[7] P. A. Basore, D. T. Rover and A. W. Smith, "PC-1D version 2: Enhanced numerical solar cell modeling," in proc. of *20th IEEE Photovolt. Special Conf.*, 1988, pp. 389-396.

[8] L. A.Verhoef and W. C. Sinke, "Minority-carrier transport in nonuniformly doped silicon-an analytical approach," I*EEE Trans. Electron Devices,* vol. 37, no. 1, pp. 210-221, Jan. 1990.

[9] L. A. Verhoef and W. C. Sinke, "New Analytical Expression for Dark Current Calculation of highly doped region in semiconductor," *IEEE Trans. Electron Devices,* vol. 44, no. 1, pp. 171-, Jan. 1997.

[10] M. R. Huqe, S. I. Reba, M. S. Uddin and M. I. B. Chowdhury, "Analytical Modeling of the Base Dark Saturation Current of Drift-Field Solar Cells Considering Auger Recombination," *Int. J. Renew. Energy Res.*, vol. 3, no. 2, pp. 420-426, 2013.

[11] D. B. M. Klaassen, J. W. Slotboom and H. C. de Graaff, "Unified apparent bandgap narrowing in n- and p-type Silicon," *Solid-State Electron.,* vol. 35, no. 2, pp. 125-129, 1992.

[12] R. J. van Overstraeten, H. J. Deman and R. P. Mertens, "Transport equations in heavy doped silicon," *IEEE Trans. Electron Devices,* vol. ED-20, no. 3, pp. 290-298, Mar. 1973.

[13] M. M. Shahidul Hassan, Orchi Hassan and M. I. B. Chowdhury, "Effect of Majority Carrier Current on the Base Transit Time of a BJT," *Journal of Electron Devices,* vol. 10, pp. 511- 514, 2011.

[14] J. G. Fossum and D. S. Lee, "A physical model for the dependence of carrier lifetime on doping density in nondegenrate silicon," *Solid-State Electron.,* vol. 25, no. 8, pp. 741-747, 1982.

[15] J. G. Fossum, "Computer-aided numerical analysis of silicon solar cells", *Solid-State Electron.*, vol. 19, pp. 269-277, 1976.

[16] J. Dziewior and W. Schmid, "Auger coefficient for highly doped and highly excited silicon," Appl. Phys. Lett., vol. 31, no. 5, pp. 346-348, May 1977.

[17] S. M. Sze, *Physics of Semiconductor Devices,* 2nd ed., New York, U.S.A.: Wiley, 1981, ch. 14, pp. 800-805.